Whole-brain connectivity dynamics reflect both task-specific and individual-specific modulation: A multitask study

Hua Xie[a,d,*], **Vince D. Calhoun**[b,c], **Javier Gonzalez-Castillo**[d], **Eswar Damaraju**[b,c], **Robyn Miller**[b], **Peter A. Bandettini**[d,e], and **Sunanda Mitra**[a]

[a]Department of Electrical and Computer Engineering, Texas Tech University, Lubbock, TX, USA

[b]The Mind Research Network, Albuquerque, NM, USA

[c]Department of Electrical and Computer Engineering, University of New Mexico, Albuquerque, NM, USA

[d]Section on Functional Imaging Methods, National Institute of Mental Health, National Institutes of Health, Bethesda, MD, USA

[e]Functional MRI Facility, National Institute of Mental Health, National Institutes of Health, Bethesda, MD, USA

Abstract

Functional connectivity (FC) has been widely used to study the functional organization of temporally correlated and spatially distributed brain regions. Recent studies of FC dynamics, quantified by windowed correlations, provide new insights to analyze dynamic, context-dependent reconfiguration of brain networks. A set of reoccurring whole-brain connectivity patterns at rest, referred to as FC states, have been identified, hypothetically reflecting underlying cognitive processes or mental states. We posit that the mean FC information for a given subject represents a significant contribution to the group-level FC dynamics. We show that the subject-specific FC profile, termed as FC individuality, can be removed to increase sensitivity to cognitively relevant FC states. To assess the impact of the FC individuality and task-specific FC modulation on the group-level FC dynamics analysis, we generate and analyze group studies of four subjects engaging in four cognitive conditions (rest, simple math, two-back memory, and visual attention task). We also propose a model to quantitatively evaluate the effect of two factors, namely, subject-specific and task-specific modulation on FC dynamics. We show that FC individuality is a predominant factor in group-level FC variability, and the embedded cognitively relevant FC states are clearly visible after removing the individual's connectivity profile. Our results challenge the current understanding of FC states and emphasize the importance of individual heterogeneity in connectivity dynamics analysis.

Keywords

FC individuality; Cognitively relevant FC state; Connectivity dynamics

---

[*]Corresponding author at: Department of Electrical and Computer Engineering, Texas Tech University, 910 Boston Avenue, Lubbock, TX 79409-3102, USA. oliver.xie@ttu.edu (H. Xie).

Introduction

Significant progress has been achieved in the assessment of functional connectivity (FC) (Horwitz, 2003) from functional magnetic resonance imaging (fMRI) time series, which is quantified as the inter-regional temporal correlation of blood oxygenation level-dependent (BOLD) signal. A wealth of findings has revealed a set of consistent (Damoiseaux et al., 2006) and highly reproducible FC patterns (Chou et al., 2012), which deepens our knowledge of the global configuration of brain networks as well as functional connections of specific brain regions and local networks (Greicius et al., 2003; Lynall et al., 2010). Until recently, most FC studies focused on static FC patterns computed using the entire scan. Nevertheless, due to the dynamic nature of human brain, it has been proposed that quantifying FC fluctuations over time may facilitate our understanding of fundamental properties of brain networks (Hutchison et al., 2013). A pipeline was proposed by Allen et al. (2014) to analyze resting-state whole-brain FC dynamics, represented by dynamic functional network connectivity (dFNC) matrices, i.e. connectivity among windowed time courses of independent component networks (ICNs) extracted via group independent component analysis (GICA). Such analyses have shown great potential in probing individual's underlying cognitive process to contrast different diagnostic groups (Damaraju et al., 2014; Rashid et al., 2016) and different levels of awareness (Barttfeld et al., 2015). In these studies, time-varying windowed correlation matrices, are analyzed via k-means clustering yielding a set of unanticipated connectivity patterns known as FC states. These FC states are found to diverge strongly from stationary connectivity patterns, and are hypothesized to reflect changes in ongoing cognitive processes during rest. However, the functional interpretation of the FC states is not well understood although there have been some links between the FC states and various aspects of drowsiness or light sleep as quantified via EEG (Allen et al., 2013).

In a recent study, we adopted a similar pipeline as proposed by Allen et al. (2014) on a multitask dataset (Gonzalez-Castillo et al., 2015). We noticed that although a high accuracy was achieved predicting ongoing tasks within individual subjects using dFNCs, the accuracy dropped significantly to near chance level when performing a preliminary group-level classification analysis. We also noted that despite being modulated to some extent by the task, dFNCs were highly predictive of an individual's identity at the group level, which was consistent with the finding by Finn et al. (2015) that the individual's connectivity profiles can be used as a 'fingerprint' to identify subjects from a large group. This evidence raises the following questions. What is the main contributor to FC variability for group-level studies? If the subject-specific FC profile, referred to as FC individuality, accounts for much more FC variability than task modulation in a group study, will we be able to observe FC states reflecting underlying cognitive processes as suggested by Allen et al. (2014)? If not, is it possible to remove FC individuality as a confounding factor to reveal cognitively relevant FC states at the group level?

To address the above questions, we designed a simple scheme by randomly selecting four subjects engaged in four different cognitive conditions to analyze a small group study with multiple cognitive processes, including resting. Next, group ICA, dFNCs extraction, and k-means clustering were applied to the data. We then compared the clustering results with task

modulation and subject identity (FC individuality) to investigate the contribution of the two factors in group-level FC dynamics. Moreover, we proposed a model to quantitatively evaluate the effect of the above-mentioned factors on FC dynamics. Our results confirmed that the FC individuality was the dominant factor in the group-level FC clustering analysis, challenging our current understanding of FC states, and emphasizing the significance of heterogeneity across individuals. Moreover, group-level cognitively relevant FC states could be extracted after removal of subject-specific FC profile, indicating that the cognition-induced FC modulation was only shadowed by the difference in the FC individuality, and such cognitively relevant FC patterns were coherent across individuals. Hence, the model we proposed might help us differentiate FC variance related to subject-specific FC profile from FC variance modulated by cognition in a group study, and improve our ability to better interpret group-level FC patterns especially for regions with considerable inter-subject variability and measure inter-subject FC difference.

Materials and methods

Data acquisition & experimental design

The fMRI data of seventeen publicly available subjects from the original study by Gonzalez-Castillo et al. (2015) were used in this study (https://central.xnat.org, project ID: FCStateClassif). One subject was excluded due to a different scanning protocol used and two more were not available due to sharing restrictions. Subjects were scanned for approximately 25 min as they engaged in four different mental tasks (math, memory, video and rest) using a Siemens 7 T MRI scanner. Each task (180 s) was repeated twice and instructions between two tasks lasted for 12 s. Imaging data were acquired with a 32-element receive coil (Nova Medical) with gradient recalled, single shot, echo planar imaging (gre-EPI) sequence with TR = 1.5 s, TE = 25 ms; FA = 50°, 40 interleaved slices; FOV = 192 mm; in-plane resolution, 2×2 mm; slice thickness, 2 mm (Fig. 1).

Data preprocessing

Functional images were preprocessed using an analysis pipeline developed at the Mind Research Network (MRN), which included SPM (http://www.fil.ion.ucl.ac.uk/spm/software/), and AFNI (https://afni.nimh.nih.gov/afni). The first four image volumes were discarded to avoid T1 equilibration effects and the remaining 1012 volumes underwent the following preprocessing steps: slice-time correction using middle slice as the reference slice; motion correction; despiking (*3dDespike*); detrending up to 8th order given the long scan time (*3dDetrend*); spatial normalization to Montreal Neurological Institute (MNI) space with voxel size of 3 mm $\times$ 3 mm $\times$ 3 mm; spatial smoothing with a Gaussian kernel (FWHM = 4 mm); and finally intensity normalization to percentage signal change by dividing each voxel's time series by its own mean intensity across time.

Data postprocessing, group ICA (GICA) & FNC estimation

The preprocessed data were further decomposed via group-level spatial ICA as streamlined in the GIFT toolbox (http://mialab.mrn.org/software/gift/), which is a data-driven method assuming a set of maximally spatially independent components and provides a more comprehensive functional parcellation of the brain imaging data (Calhoun and Adali, 2012).

We adopted a similar pipeline as proposed by Allen et al. (2014) with a relatively high model order (number of components) equal to 100. Subject-specific data reduction retained 120 principal components and group data reduction kept 100 principal components using the expectation maximization (EM) algorithm. The Infomax ICA algorithm was repeated 20 times using ICASSO (http://www.cis.hut.fi/projects/ica/icasso) with random initialization, and the most central run was selected to mitigate variability due to the stochastic ICA runs. Subject-specific spatial maps and time courses (TCs) were estimated using the GICA1 back reconstruction method based on PCA compression and projection (Erhardt et al., 2011). A subset of 61 independent component networks (ICNs) were manually identified in contrast to imaging artifacts and noise, based on the criteria that ICNs should show peak activations in grey matter, and should have TCs dominated by low-frequency or task-frequency fluctuations. The chosen TCs underwent motion-related variance regression (6 motion parameters and the first derivatives).

The whole TCs were then bandpass filtered with a 6th order Butterworth bandpass filter (0.01–0.18 Hz) consistent with the bandwidth used in the original study (Gonzalez-Castillo et al., 2015). The lower cut-off frequency was set to 0.01 Hz to remove trends associated with scanner drift. The upper cut-of frequency was chosen to be 0.18 Hz to avoid the confounds arising from task motor responses. These were the most frequent during the math task (one button press every five seconds, 0.2 Hz). Then the static functional network connectivity (sFNC) patterns were calculated as pairwise Pearson's correlations between TCs from all chosen components, and resulted in a 61×61 matrix. The four task-specific sFNC patterns (rest, memory, math and video) were computed using time courses of two blocks of the same task ($120 + 120 = 240$ TRs). The whole-scan sFNC patterns were calculated using all 1012 time points as shown in Fig. 2.

Dynamic functional network connectivity (dFNC) patterns reflect windowed FNC snapshots at different time instances. The windowed TCs were estimated using a sliding temporal window (Tukey window) with a width of 30 TRs (45 s) sliding in steps of 1 TR shown in Fig. 2. The windowed TCs were then bandpass filtered based on window length to remove spurious fluctuations (0.0222–0.18 Hz) as suggested by Leonardi and Van De Ville (2015). The pairwise correlations between filtered TCs were computed, yielding $1012–30 = 982$ dFNCs, each of which was a 61×61 windowed correlation matrix. As a relatively short window length may not provide enough information to characterize the full correlation matrix, we adopted the graphical LASSO method by placing a penalty on the L1 norm of the precision matrix (inverse correlation matrix) to promote sparsity (Friedman et al., 2008). Both dFNC and sFNC matrices were Fisher transformed, and then vectorized from a matrix to a feature vector with $61 \times (61-1)/2 = 1830$ features.

FC individuality vs cognitive modulation

To determine whether the FC states revealed by k-means clustering in resting-state studies are related to underlying cognitive process, and to compare the influence of FC individuality and cognitive modulation of the FC dynamics in a group study, we designed a simple scheme to construct a group study with known underlying cognitive modulation and subject identity. We randomly selected four subjects out of thirteen good performers according to

our preliminary results and the original study (Gonzalez-Castillo et al., 2015) to ensure windowed FNC snapshots (dFNCs) stemmed from task engagement, and were predictive of the ongoing task. Then we randomly sampled 200 purely task-related dFNCs (windows with no overlap with introduction periods between two tasks) from each subject equally divided in terms of task modulation, resulting in a series of 800 dFNCs equally divided in terms of subject identity and task modulation (200 per task/subject). Then k-means clustering was applied on the dFNCs with number of clusters set to four, maximum number of iteration to 1000, number of replicates to 50, and Pearson's correlation as the distance measure. We compared the k-means clustering results against the subject identity and task modulation in terms of classification accuracy to evaluate classification performance. If the resultant partition agrees much better with subject identity than task modulation, then the group-level FC dynamics and the FC states are dominated by the difference in subject-specific FC patterns. If the reverse is true, the difference in FC individuality is not a key factor in the group analysis and resultant FC states reflect the ongoing task. As the k-means clustering is an unsupervised technique, it could not be used to label resulting clusters (e.g. cluster one = math). All possible ways of correspondence between the clusters and the labels were sorted based on the number of matches, and the one yielding the most matches was used to calculate the classification accuracy. Since such estimation might be over-optimistic, we also adopted the adjusted rand index (ARI) (Steinley, 2004) as an external clustering validation technique for unlabeled clusters. The ARI ranges from 1 to below 0, with 1 indicating perfect recovery of the known clusters, 0 indicating chance level performance, and smaller than 0 indicating worse than chance. An ARI greater than 0.9 means excellent recovery; ARI between 0.8 and 0.9 means good recovery, ARI between 0.65 and 0.8 means moderate recovery; ARI smaller than 0.65 means poor recovery (Steinley, 2004).

We also proposed the following multiple regression model to quantitatively assess the effect of the two factors and better explain the outcome of the group studies:

$$dFNC(i, w) = \sum_{i=1}^{\# sub} b_{indiv}(i, w) \times FNC_{indiv}(i) + \sum_{j=1}^{\# task} b_{cog}(j, w) \times FNC_{cog}(j) + \varepsilon(i, w), \quad (1)$$

where $dFNC(i, w)$ is the windowed FNC snapshot of the wth window from subject i; $FNC_{indiv}(i)$ is the FC individuality of subject i, characterized by the individual's whole-scan sFNC pattern; $FNC_{cog}(j)$ is the group-level task-induced FC modulation by task j, computed using all the time points from task j and averaged across subjects; $\varepsilon(i, w)$ is the error term.

To explain the outcome of the group studies consisting of four tasks and four subjects, a paired t-test was used on the variance explained by the four FNC_{indiv} regressors and four FNC_{cog} regressors.

Removal of FC individuality

To determine whether the task-induced FC modulation was just obscured by the FC individuality, and could be revealed after the removal of FC individuality, the dFNCs of the

thirteen good performers were regressed on the FC individuality quantified with the whole-scan sFNC pattern after vectorization of the sFNC and dFNC patterns.

$$dFNC(i, w) = b_{indiv}(i, w) \times FNC_{indiv}(i) + dFNC\_IR(i, w), \quad (2)$$

where $dFNC(i, w)$ is the windowed FNC snapshot of the wth window from subject i; $FNC_{indiv}(i)$ is the FC individuality of subject i, characterized by the individual's whole-scan sFNC pattern; and the residual term $dFNC\_IR(i, w)$ is the individuality-removed dFNC.

In other words, by regressing out FC individuality (FNC_{indiv}), we hoped to remove the FC pattern common to a given subject regardless of the condition, to boost contrast of task-specific dFNC patterns at the group level. Next the residual data $dFNC\_IR(i, w)$, the individuality-removed dFNCs, were taken as the input for k-means clustering. The classification accuracy and ARI were computed the same way as in *FC individuality vs cognitive modulation*. We were interested to see if the FC states from k-means clustering reflected more on ongoing tasks after removing variance related to FC individuality.

Additionally, we wanted to investigate how to better characterize and remove the subject-specific FC profile while retaining task-induced modulation on FC dynamics. We replaced the whole-scan sFNC pattern with various other sFNC patterns, such as the resting-state sFNC pattern and other task-specific sFNC patterns (math, video and memory), to investigate if any of those or combination of those could be more informative of the FC individuality. Since k-means classification accuracy or ARI is only an indirect measure of FC individuality, we also proposed a more direct measure called observability ratio (OR) to quantify our ability to remove FC individuality as well as highlight task-induced FC modulation defined as the following:

$$OR = \frac{mean\,[S_{task}(j) - S_{GM}]}{mean\,[S_{indiv}(i) - S_{GM}]}, \quad (3)$$

where $S_{task}(j)$ is the within-task similarity reflecting the coherence of FC modulation of a given task j across subjects; and $S_{indiv}(i)$ is within-subject FC similarity of subject i showing the influence of the FC individuality on the FC dynamics; S_{GM} is the global mean of the similarity of all dFNCs across all subjects and tasks. Similarity was quantified by correlating two vectorized dFNCs using Pearson's correlation. Higher OR indicates better observability of cognitively relevant FC states in a group study.

All $716 \times 13 = 9308$ (#window $\times$ #good performer) purely task-related dFNCs were concatenated and similarities were calculated, resulting in a 9308×9308 similarity matrix. S_{task} was calculated by averaging over all dFNC similarity pairs from the same task and S_{indiv} was calculated by averaging over all pairs from the same subject as an example can be found in Fig. 3.

Results

Windowed FNC snapshots are highly predictive of subject identity

To evaluate how well windowed dFNCs can predict subject identity, we compared all windowed dFNC snapshots of all subjects against the FC individuality (as computed using the whole scan) of each of our 17 participants. The subject whose FC individuality was the most similar to the dFNC under study was marked as the predicted identity for that particular window of time of that particular scan. In this context, similarity was computed as the Pearson's correlation coefficient between vectorized dFNC and sFNC matrices. Since there were 982 windowed FNC snapshots per subject, the prediction accuracy was calculated as the number of correct identifications divided by the total number of windows. An average of 98.49% prediction accuracy was achieved for all 17 subjects. Subject-specific prediction accuracy is shown in Fig. 4. For many subjects, this method yielded 100% accuracy in subject identification. The lowest accuracy occurred for Subject 10 (95.11%). This suggests that FC dynamics computed on the scale of tens of seconds can be used to predict individual's identity with almost perfect accuracy, despite the task modulation. In other words, subject-specific FC profiles are embedded in the transient FC dynamics.

FC individuality dominates clustering results

To evaluate to what degree the FC states in resting-state are related to the underlying cognitive modulation, we constructed a group study with four subjects randomly chosen from thirteen good performers and the total 800 dFNCs were equally split in terms of task modulation and subject identity (200 dFNCs per task/subject). K-means clustering results of 100 repetitions suggest that the FC individuality, quantified by an individual's whole-scan sFNC pattern, is almost solely responsible for the resultant FC states, as suggested by the histogram of classification accuracies of all repetitions shown in Fig. 5.

To quantitatively analyze the group-level FC dynamics and the outcomes of k-means clustering, we implemented the multiple regression model as described in Eq. (1). Four subjects were randomly chosen from all 17 subjects and 200 purely task-related dFNCs were randomly sampled from each subject. Four task-specific sFNC patterns and four subject-specific sFNC profiles (whole-scan sFNC pattern) were used as regressors to fit 800 dFNCs. The above steps were repeated 500 times, and a paired t-test on variance explained by subject identity and task modulation confirmed the FC individuality accounted for significantly more variability than task modulation in group-level FC dynamics (p = 2.39×10^{-15}).

Investigation of FC individuality removal

One of our goals was to determine whether the task-induced FC modulation could be separated from FC individuality in order to better reveal task effects. Hence, we regressed out FC individuality from the dFNC time series and applied k-means clustering on the regressed dFNCs. After regressing out the FC individuality from dFNCs, the FC states were found to be much more relevant to the task modulation. To demonstrate this, 32 dFNC snapshots randomly selected from the first four subjects (8 dFNCs per subject/task) were projected to a 2-D space using a high-dimensional data visualization tool t-SNE (Van Der

Maaten and Hinton, 2008) (https://lvdmaaten.github.io/tsne/). As shown in Fig. 6(a), the raw dFNCs were clustered based on the subject identity and the regressed (individuality-removed) dFNCs were clustered according to task modulation as illustrated in Fig. 6(d), suggesting originally obscured task-induced FC patterns appear to be better captured after removal of FC individuality.

Moreover, the k-means clustering results over 100 repetitions are compared against subject identity and task modulation, and the histogram of classification accuracies is shown in Fig. 7. After the removal of FC individuality, the agreement between FC states and the task modulation increased significantly from 29.88% to 90.43% in terms of the average classification accuracy. On the contrary, the average classification accuracy based on subject identity notably dropped from almost perfect (93.67%) to almost chance level (30.05%).

The ARI was also computed as an external clustering validation technique for unlabeled clusters. The ARIs of the 100 repetitions summarized in Table 1 showed how ARI changed before and after removal of FC individuality. The frequency of excellent/good/moderate recovery of task modulation increased remarkably after the FC individuality removal, which was consistent with our observation in terms of classification accuracy that the FC states were highly predictive to ongoing tasks after regressing out the subject-specific FC pattern.

Furthermore, we explored various ways to characterize FC individuality to investigate if any task-specific FC pattern or combination of some (e.g. rest + math sFNC pattern) could be more informative about individual's FC profile. We calculated the *OR* of the regressed dFNCs to quantitatively analyze how distinctive and consistent cognitive modulation was across subjects after regressing on different representation of FC individuality. The one with highest *OR* would yield best classification performance and could be used to unravel the cognitively relevant FC patterns shadowed by FC individuality. We calculated all 15 possible combinations of sFNC patterns by using time points from those mental states and summarized the OR_s in the Table 2.

We also conducted experiments to compare the performance of removing FC individuality using three-task sFNC patterns and the four-task sFNC pattern. The ARI after regression was shown in Fig. 8 and the four-task sFNC pattern yielded significantly higher ARI than three-task sFNC combinations ($p < 0.01$, Bonferroni adjusted) except for the three-task sFNC pattern without rest ($p = 0.253$, Bonferroni adjusted). The ARI was consistent with the OR_s in Table 2, indicating that averaging over multiple tasks (four-task sFNC pattern) provided better characterization of FC individuality leading to more cognitively relevant partitions.

Fig. 9 shows the group averaged whole-scan sFNC pattern. ICNs were grouped into eight brain networks: sensorimotor (SM), visual (VIS), subcortical (SC), auditory (AUD), cognitive control (CC; referring loosely to the planning, monitoring, and adapting one's behavior), default-mode (DM), salience network (SN) and attentional network (ATTN). This was done based on the parcellation scheme in Allen et al. (2014) and Vergara et al. (2016). Qualitatively, it can be observed that group averaged sFNC pattern is not that different from static FC patterns during rest. Stronger connectivity was found for within-network

connections than for between-network connections, while no obvious anticorrelation pattern between DM and other networks as during rest is present.

Effect of individuality removal on FC dynamics

To further investigate how FC individuality removal helped reduce the inter-subject connectivity variability besides k-means clustering and *OR*, we analyzed the group-level FC variance of the dFNCs time series of thirteen good performers before and after FC individuality removal.

The dFNCs were first grouped based on task; and then group-level dFNC variance was calculated within each task before and after FC individuality removal. Finally, the percentage change of such variance was averaged across tasks. Our result indicates there was a significant decrease in variance of group-level FC dynamics across the whole brain (on average accounting for 13.32% reduction in variance). Fig. 10 shows the decrease in variance for a selective group of ICNs that have the highest decrease in FC variability within each functional network. Highest decreases were observed in the ICNs covering the ventral frontal cortices, including the right middle frontal cortex (R MiFG, ICN 57) and the right inferior frontal gyrus (R IFG, ICN 58). Additional ICNs with highest decreases on variance include those on dorsal frontoparietal cortex such as superior parietal lobule (SPL, ICN 60). Moreover, the most significantly changed connection was that between R MiFG and R IFG; whose group-level FC dynamics variance decreased by 45.84%. The least changed ICNs were found to lie primarily within primary visual and unimodal somatosensory association areas, e.g. postcentral gyrus (PoCG), supramarginal gyrus (SMG), left middle occipital gyrus (L MOG) and right superior occipital gyrus (R SOG).

Network-level changes in variance of FC dynamics following individuality removal are reported in Table 3. Sensorimotor, visual, auditory and default-mode networks are among those with the least decrease in variance. Moreover, subcortical and cognitive control network showed a moderate level of decrease in variability. The salience network and attentional network showed the highest decrease among all (i.e., contained the most traces of individuality).

To make sure that task-specific FC dynamics, i.e. FC fluctuations across time within a given individual, were not removed during the FC individuality regression, we computed the task-related FC dynamics in terms of the variance of each FC edge strength across time within each individual. We found task-related FC dynamics were largely unaffected as an average of 97.01% task-related FC variance was preserved after the regression, and task-related FC dynamics patterns before and after regression were highly similar with an average of 0.955 in terms of Pearson's correlation. Taken together, those observations explain the higher *OR* and the higher clustering accuracy achieved after regression due to the preserved contrast across conditions and removal FC dynamics associated with inter-subject FC individuality difference.

Discussion

Every human being is one of a kind. Despite long recognized high individual variability within healthy individuals in terms of activation patterns during tasks (Grabner et al., 2007) and functional connectivity at rest (Mueller et al., 2013); the considerable heterogeneity present across subjects is usually overlooked in group studies in order to draw population-level inference. It was demonstrated by Finn et al. (2015) that an individual's whole-brain FC pattern, which was calculated using a number of volumes ranging from 100 to 1100, could be used as a 'fingerprint' to identify individuals regardless of condition (task or rest). Based on that result, it was argued by the authors that a substantial portion of the brain connectivity pattern was unique to each individual. We found that such identification ability persisted even on the scale of tens of seconds by comparing the windowed FC patterns across four cognitive conditions with all individuals' FC profiles. The windowed FC patterns computed using only 30 time points were highly predictive of subject identity instead of task modulation, highlighting the considerable difference between the FC individuality, i.e. subject-specific FC profile.

Hence, to investigate how important a role the FC individuality plays in a group-level analysis, we constructed a series of group studies with known subject identity and cognitive modulation and proposed a model to decompose the group-level FC dynamics into two terms: subject-specific FC profile and task-specific FC modulation. By assessing the effect of FC individuality and cognitive modulation using a multitask dataset, we demonstrated that the variability of group-level FC dynamics was largely driven by FC individuality instead of task modulation. Our results reaffirm the existence of an "intrinsic" standard architecture of functional brain organization during rest and task (Cole et al., 2014). Our conclusion is also supported by the finding by Calhoun et al. (2008) where two sets of networks were identified as associated with rest and auditory oddball task for both patients and healthy controls, and their spatial patterns were only slightly different between the two conditions. However, by highlighting the inter-subject difference and connectivity dynamics, we further showed that despite FC dynamics being largely determined by FC individuality, the hidden task-induced FC modulation could still be revealed after the removal of subject-specific FC pattern to predict ongoing cognitive process in a group study. Hence our proposed model of separating the group-level FC dynamics into two components as in Eq. (1) better captures cognitively relevant FC states in a group-level analysis within the limited scope of our study. Moreover, our findings challenge the current understanding of FC states during rest (Allen et al., 2014) by raising a potential concern regarding how well FC states during rest reflect underlying cognitive processes without taking FC individuality into consideration; and emphasize the importance of individual heterogeneity in connectivity analysis, which needs to be more systematically and quantitatively analyzed.

FC individuality characterization

FC individuality is defined as the FC pattern specific to a subject regardless of task engagement, which is a similar concept as the intrinsic FC structure shared by both rest and task (Cole et al., 2014). FC individuality may be important for further understanding individual differences such as fluid intelligence (Finn et al., 2015), but may not be as

informative with respect to engagement in a given mental process. We observed improved group-level clustering accuracy after removing FC individuality when decoding the brain state using group-level FC dynamics. A similar argument was made by Poldrack (2006) to predict mental processes using activation patterns. In that work, it was argued that if a given region is activated for many different mental processes, then activation in that region would not be very informative to predict the engagement of a specific mental process.

To better remove the variance related to the subject-specific FC profile from group-level FC dynamics, we explored different characterizations of FC individuality by using a combination of the static task-specific FC patterns instead of the whole-scan sFNCs. Among all possible combinations, we found that removing FC individuality characterized by whole-scan sFNCs led to the highest accuracy of task prediction as well as the observability ratio (OR) which quantifies the visibility of task modulation on FC patterns. This is consistent with a previous finding by Finn et al. (2015), where a task or rest dataset by itself yielded lower accuracy identifying subjects than combining the two together; suggesting the individual's FC 'fingerprint' might be better captured by including multiple conditions. Although resting-state FC pattern presumably characterizes the intrinsic functional network configuration occurring across many (or all) brain states (Fox and Raichle, 2007), our results suggested that resting-state FC patterns might not fully reflect the subject-specific FC profile given its worst k-means clustering performance and OR among all representations of FC individuality. It should be also noted that the 3-task sFNC pattern without rest (Memory + Video + Math) was only slightly (but not statistically significantly) worse than whole-scan sFNC pattern but much better than the other 3-task sFNC patterns ($p < 0.01$, Bonferroni adjusted), all of which included rest. Furthermore, resting-state connectivity patterns were shown to be negatively correlated with task performance in our recent work (Xie et al., 2017). We argue that "rest" can still be considered an unconstrained task (Buckner et al., 2013) or an opposite of a task (so-called task-negative) (Weissman et al., 2006), but not necessarily a consistent reference (subject-specific and task-neutral) to enhance contrast against various task conditions at the group level or to compare the subject-specific FC profile. Hence, the static resting-state FC pattern might not necessarily better capture the intrinsic generic functional organization of an individual's brain 'fingerprint' than a static task-specific FC pattern. A similar argument has been made by Finn et al. (2017) that the resting state may not be the optimal brain state for measuring individual FC variability. Intuitively, this is understandable given the resting state is largely unconstrained/ambiguous and the possibility of existence of multiple sub mental states during rest (Calhoun and Adali, 2016), which may not be reflected by the static resting-state FC pattern. All these pieces of evidence raise our concern regarding whether the static resting-state FC pattern is the best characterization for FC individuality, since the considerable inter-subject resting-state FC variability has been shown to be non-uniformly distributed across brain networks (Mueller et al., 2013) and only partially reflects anatomical networks (Goñi et al., 2014). It might be worth investigating if the time-averaged FC pattern from relatively long multitasks scans better captures the brain's generic configuration, as longer scans improve the stability of connectivity pattern (Gonzalez-Castillo et al., 2014). One additional component that may contribute to subject specific variance is the residual physiological noise not fully accounted for by our current pre-processing pipeline. Additional pre-processing steps targeting

physiological noise, such as RETROICOR (Glover et al., 2000) and CompCorr (Behzadi et al., 2007), may help reduce the contribution of physiological noise to subject individuality, and should be the focus of additional research. It is also noteworthy that we are limited to a small set of tasks when characterizing FC individuality, thus the FC individuality in our study only captured FC modulation across a few task domains. Hence, it would be interesting to investigate whether it is possible to develop a standardized set of naturalistic tasks covering a wider cognitive scope to better characterize FC individuality and better understand inter-subject FC differences, and whether it might resemble more of individual's anatomical connectivity pattern.

FC individuality removal in cognitive studies

FC individuality may be very helpful for clinical studies contrasting different diagnostic populations, where group-averaged FC pattern is altered significantly for patients with neuropsychiatric disorders (Damaraju et al., 2014; Garrity et al., 2007; Rashid et al., 2016; Zhang and Raichle, 2010). However, it is not clear how FC individuality would affect the interpretation of group-level FC patterns and outcome of other connectivity-based approaches in cognitive studies, where the cognitively relevant FC modulation might be subtle compared to the variability associated with FC individuality. In this scenario, the difference between subject-specific connectivity patterns might prevent us from drawing consistent group-level inferences on the task-induced FC modulation pattern, especially in highly variable regions. For example, it is more likely to get a significant result in areas with low inter-subject variability such as primary sensory or motor cortex and less likely to get a significant result in areas with high inter-subject variability (Mueller et al., 2013). In that study, it has been also shown that the regions predicting individual differences in cognitive and behavioral are predominantly located in regions with high inter-subject FC variability. We argue that a large portion of inter-subject FC variability within the same task may be caused by the difference in the FC individuality, and FC individuality removal might help us capture task-induced FC modulation more faithfully, which may be very critical to build FC-based dictionaries proposed by Gonzalez-Castillo et al. (2015).

In this study, we found the ICNs with most overall change in group-level FC dynamics after removing FC individuality belong to ventral frontal cortices (e.g. R MiFG and R IFG) and dorsal frontoparietal cortex (e.g. SPL) indicating greater inter-subject connectivity variability within those regions, while the least changed ICNs were identified as primary visual and unimodal somatosensory association areas such as SMG, PoCG, L MOG, and R SOG, suggesting relatively less inter-subject connectivity variability. Our findings agree with the previous literatures, as FC variability during rest was reported to be highest in frontal, temporal, and parietal association cortex areas while lowest in unimodal sensory and motor cortices (Mueller et al., 2013); and the medial frontal and frontoparietal networks were found to yield highest individual identification power suggesting the greatest inter-subject FC difference in those networks (Finn et al., 2015).

It is worth noting that the regions showing greatest decrease in group-level FC dynamics have shown to be related to attention, such as R MiFG (Japee et al., 2015), R IFG (Hampshire et al., 2010) and SPL (Wang et al., 2015). It has been proposed that the right

hemisphere dominant ventral frontal cortex, including the MiFG, IFG, together with frontal operculum and anterior insula, is part of Ventral Attention Network (VAN) and they play important roles in the sensory-driven exogenous bottom-up attention (Corbetta et al., 2008). On the other hand, as a part of the dorsal attention network (DAN), SPL is responsible for the top-down control of visual attention driven by endogenous stimuli. Moreover, the dorsal and ventral attention networks are believed to converge at right MiFG, as it interrupts endogenous attentional processes and reorient attention to the exogenous stimulus (Japee et al., 2015), which is supported by our finding that R MiFG being the most variable ICN allowing for flexible control of both endogenous and exogenous stimuli. Taken together, the fact that the FC individuality is so much shaped by above-mentioned key hubs associated with attention is worth further investigation, which may deepen our understanding of individual's behavior and trait and functional organization within the DAN and VAN (Vossel et al., 2014).

On the sliding window correlation approach

The accuracy of the sliding window correlation (SWC) approach to measure FC dynamics has been discussed widely in recent literatures (Hindriks et al., 2016; Kudela et al., 2017; Leonardi and Van De Ville, 2015; Shakil et al., 2016; Thompson and Fransson, 2016). For example, to minimize spurious fluctuations in FC dynamics, it has been suggested to use as 1/WL (WL = 30TRs = 45 s) as the low-cutoff frequency for filtering prior to estimating dFNCs (Leonardi and Van De Ville, 2015). It is claimed by Shakil et al. (2016) that due to lack of the ground truth in the resting-state fMRI data, the actual FC dynamics, number of states, and state transitions are all unknown, and therefore results difficult to validate. However, the use of a continuous multitask experimental design, such as the one presented here and by Gonzalez-Castillo et al. (2015), provides the experimenter with initial ground truth for most of these variables by trying to enforce mental states via tasks. Within such framework, it is possible to test that to which degree FC states reflect ongoing cognition at short temporal scales (under the assumption of subject's compliance). It is also shown that the SWC approach can perform well when the underlying network is changing very slowly (Shakil et al., 2016), which is the case for our experimental setup as each task lasts for 120TRs = 180 s.

Statistical tests were developed by to detect FC dynamics using the SWC approach during rest and are validated using simulation and real data from macaque and human (Hindriks et al., 2016). In that study, it is recommended that the optimal window length should be around $\tau/3$, where τ is the characteristic timescale of FC fluctuations, or 50 s without the knowledge about the true correlation timescale. Albeit the task-related dFNC patterns were quite distinct in our study, we tested the standard deviation of real dFNC time series against a null distribution obtained via phase randomization which scrambled dynamic interrelationships while preserving the static correlation structure of real data (Hindriks et al., 2016). As anticipated, the standard deviation of all connectivities were significantly greater than the 95th percentile of the null distribution. Despite the uncertainty associated with the dynamics estimation via SWC approach (Hindriks et al., 2016; Kudela et al., 2017), dFNCs of different tasks still obviously distinguished from each other and were predictive to task engagement after FC individuality removal. In the future, we will further investigate the

possibility of improving the stability of FC dynamics estimation by adding an additional Box–Cox transformation after Fisher transformation (Thompson and Fransson, 2016).

Conclusion

In this study, we evaluated the subject-specific and task-specific modulation on FC dynamics with a continuous multitask dataset (rest, simple math, two-back memory, and visual attention task) and proposed a model to decompose the group-level FC dynamics in terms of subject-specific FC profile (FC individuality) and cognitive modulation. We found that the FC individuality primarily contributes to the group-level FC dynamics across all four cognitive conditions. Regressing out the FC individuality characterized as the whole-scan sFNC pattern better removed subject-specific FC structure shared across different tasks. Regressing out the FC individuality also preserved the contrast of task-specific FC patterns, enabling the identification of the ongoing cognitive processes using FC dynamics at the group level. Our work challenges the current understanding of FC states during rest and suggests that FC states are comprised of multiple separable components. This study also highlights the importance of addressing the FC individuality difference in exploring the task-related or resting-state FC characteristics.

Acknowledgments

References

Allen E, Eichele T, Wu L, Calhoun V. EEG signatures of functional connectivity states. Hum Brain Mapp. 2013; 1:2012.doi: 10.1007/s10548-017-0546-2

Allen EA, Damaraju E, Plis SM, Erhardt EB, Eichele T, Calhoun VD. Tracking whole-brain connectivity dynamics in the resting state. Cereb Cortex. 2014; 24:663–676. DOI: 10.1093/cercor/bhs352 [PubMed: 23146964]

Barttfeld P, Uhrig L, Sitt JD, Sigman M, Jarraya B, Dehaene S. Signature of consciousness in the dynamics of resting-state brain activity. Proc Natl Acad Sci USA. 2015; 112:887–892. DOI: 10.1073/pnas.1418031112 [PubMed: 25561541]

Behzadi Y, Restom K, Liau J, Liu TT. A component based noise correction method (CompCor) for BOLD and perfusion based fMRI. Neuroimage. 2007; 37:90–101. DOI: 10.1016/j.neuroimage.2007.04.042 [PubMed: 17560126]

Buckner RL, Hrienen FM, Yeo TBT. Opportunities and limitations of intrinsic functional connectivity MRI. Nat Rev Neurosci. 2013; 16:832–837. DOI: 10.1038/nn.3423

Calhoun VD, Kiehl KA, Pearlson GD. Modulation of temporally coherent brain networks estimated using ICA at rest and during cognitive tasks. Hum Brain Mapp. 2008; 29:828–838. DOI: 10.1002/hbm.20581 [PubMed: 18438867]

Calhoun VD, Adali T. Multisubject independent component analysis of fMRI: a decade of intrinsic networks, default mode, and neurodiagnostic discovery. IEEE Rev Biomed Eng. 2012; 5:60–73. DOI: 10.1109/RBME.2012.2211076 [PubMed: 23231989]

Calhoun VD, Adali T. Time-varying brain connectivity in fMRI data: whole-brain data-driven approaches for capturing and characterizing dynamic states. IEEE Signal Process Mag. 2016; 33:52–66. DOI: 10.1109/MSP.2015.2478915

Chou YH, Panych LP, Dickey CC, Petrella JR, Chen NK. Investigation of long-term reproducibility of intrinsic connectivity network mapping: a resting-state fMRI study. Am J Neuroradiol. 2012; 33:833–838. DOI: 10.3174/ajnr.A2894 [PubMed: 22268094]

Cole MW, Bassett DS, Power JD, Braver TS, Petersen SE. Intrinsic and task-evoked network architectures of the human brain. Neuron. 2014; 83:238–251. DOI: 10.1016/j.neuron.2014.05.014 [PubMed: 24991964]

Corbetta M, Patel G, Shulman GL. The reorienting system of the human brain: from environment to theory of mind. Neuron. 2008; 58:306–324. DOI: 10.1016/j.neuron.2008.04.017 [PubMed: 18466742]

Damaraju E, Allen EA, Belger A, Ford JM, McEwen S, Mathalon DH, Mueller BA, Pearlson GD, Potkin SG, Preda A, Turner JA, Vaidya JG, Van Erp TG, Calhoun VD. Dynamic functional connectivity analysis reveals transient states of dysconnectivity in schizophrenia. NeuroImage Clin. 2014; 5:298–308. DOI: 10.1016/j.nicl.2014.07.003 [PubMed: 25161896]

Damoiseaux JS, Rombouts SARB, Barkhof F, Scheltens P, Stam CJ, Smith SM, Beckmann CF. Consistent resting-state networks across healthy subjects; Proc Natl Acad Sci USA. 2006. 103

Erhardt EB, Rachakonda S, Bedrick EJ, Allen EA, Adali T, Calhoun VD. Comparison of multi-subject ICA methods for analysis of fMRI data. Hum Brain Mapp. 2011; 32:2075–2095. DOI: 10.1002/hbm.21170 [PubMed: 21162045]

Finn ES, Shen X, Scheinost D, Rosenberg MD, Huang J, Chun MM, Papademetris X, Todd Constable R. Functional connectome fingerprinting: identifying individuals using patterns of brain connectivity. Nat Neurosci. 2015; 18:1–11. DOI: 10.1038/nn.4135 [PubMed: 25547471]

Finn ES, Scheinost D, Finn DM, Shen X, Papademetris X, Constable RT. Can brain state be manipulated to emphasize individual differences in functional connectivity?. Neuroimage. 2017.

Fox MD, Raichle ME. Spontaneous fluctuations in brain activity observed with functional magnetic resonance imaging. Nat Rev Neurosci. 2007; 8:700–711. DOI: 10.1038/nrn2201 [PubMed: 17704812]

Friedman J, Hastie T, Tibshirani R. Sparse inverse covariance estimation with the lasso. Biostatistics. 2008; 9:432–441. DOI: 10.1093/biostatistics/kxm045 [PubMed: 18079126]

Garrity AG, Pearlson GD, McKiernan K, Lloyd D, Kiehl KA, Calhoun VD. Aberrant "default mode" functional connectivity in schizophrenia; Am J Psychiatry. 2007. 164

Glover GH, Li TQ, Ress D. Image-based method for retrospective correction of physiological motion effects in fMRI: retroicor. Magn Reson Med. 2000; 44:162–167. DOI: 10.1002/1522-2594(200007)44:1<162::AID-MRM23>3.0.CO;2-E [PubMed: 10893535]

Goñi J, van den Heuvel MP, Avena-Koenigsberger A, Velez de Mendizabal N, Betzel RF, Griffa A, Hagmann P, Corominas-Murtra B, Thiran J-P, Sporns O. Resting-brain functional connectivity predicted by analytic measures of network communication; Proc Natl Acad Sci USA. 2014. 111

Gonzalez-Castillo J, Handwerker DA, Robinson ME, Hoy CW, Buchanan LC, Saad ZS, Bandettini PA. The spatial structure of resting state connectivity stability on the scale of minutes. Front Neurosci. 2014; 8:1–19. DOI: 10.3389/fnins.2014.00138 [PubMed: 24478622]

Gonzalez-Castillo J, Hoy CW, Handwerker Da, Robinson ME, Buchanan LC, Saad ZS, Bandettini Pa. Tracking ongoing cognition in individuals using brief, whole-brain functional connectivity patterns. Proc Natl Acad Sci USA. 2015; 112:8762–8767. DOI: 10.1073/pnas.1501242112 [PubMed: 26124112]

Grabner RH, Ansari D, Reishofer G, Stern E, Ebner F, Neuper C. Individual differences in mathematical competence predict parietal brain activation during mental calculation. Neuroimage. 2007; 38:346–356. DOI: 10.1016/j.neuroimage.2007.07.041 [PubMed: 17851092]

Greicius MD, Krasnow B, Reiss AL, Menon V. Functional connectivity in the resting brain: a network analysis of the default mode hypothesis; Proc Natl Acad Sci USA. 2003. 100

Hampshire A, Chamberlain SR, Monti MM, Duncan J, Owen AM. The role of the right inferior frontal gyrus: inhibition and attentional control. Neuroimage. 2010; 50:1313–1319. DOI: 10.1016/j.neuroimage.2009.12.109 [PubMed: 20056157]

Hindriks R, Adhikari MH, Murayama Y, Ganzetti M, Mantini D, Logothetis NK, Deco G. Can sliding-window correlations reveal dynamic functional connectivity in resting-state fMRI? Neuroimage. 2016; 127:242–256. DOI: 10.1016/j.neuroimage.2015.11.055 [PubMed: 26631813]

Horwitz B. The elusive concept of brain connectivity. Neuroimage. 2003; 19:466–470. DOI: 10.1016/ S1053-8119(03)00112-5 [PubMed: 12814595]

Hutchison RM, Womelsdorf T, Allen EA, Bandettini PA, Calhoun VD, Corbetta M, Della Penna S, Duyn JH, Glover GH, Gonzalez-Castillo J, Handwerker DA, Keilholz S, Kiviniemi V, Leopold DA, de Pasquale F, Sporns O, Walter M, Chang C. Dynamic functional connectivity: promise, issues, and interpretations. Neuroimage. 2013; 80:360–378. DOI: 10.1016/j.neuroimage. 2013.05.079 [PubMed: 23707587]

Japee S, Holiday K, Satyshur MD, Mukai I, Ungerleider LG. A role of right middle frontal gyrus in reorienting of attention: a case study. Front Syst Neurosci. 2015; 9:23.doi: 10.3389/fnsys. 2015.00023 [PubMed: 25784862]

Kudela M, Harezlak J, Lindquist MA. Assessing uncertainty in dynamic functional connectivity. Neuroimage. 2017; 149:165–177. DOI: 10.1016/j.neuroimage.2017.01.056 [PubMed: 28132931]

Leonardi N, Van De Ville D. On spurious and real fluctuations of dynamic functional connectivity during rest. Neuroimage. 2015; 104:430–436. DOI: 10.1016/j.neuroimage.2014.09.007 [PubMed: 25234118]

Lynall M, Bassett DS, Kerwin R, Mckenna PJ, Müller U, Bullmore E. Functional connectivity and brain networks in schizophrenia. J Neurosci. 2010; 30:9477–9487. DOI: 10.1523/JNEUROSCI. 0333-10.2010.Functional [PubMed: 20631176]

Mueller S, Wang D, Fox MD, Yeo BTT, Sepulcre J, Sabuncu MR, Shafee R, Lu J, Liu H. Individual variability in functional connectivity architecture of the human brain. Neuron. 2013; 77:586–595. DOI: 10.1016/j.neuron.2012.12.028 [PubMed: 23395382]

Poldrack RA. Can cognitive processes be inferred from neuroimaging data? Trends Cogn Sci. 2006; 10:59–63. DOI: 10.1016/j.tics.2005.12.004 [PubMed: 16406760]

Rashid B, Arbabshirani MR, Damaraju E, Cetin MS, Miller R, Pearlson GD, Calhoun VD. Classification of schizophrenia and bipolar patients using static and dynamic resting-state fMRI brain connectivity. Neuroimage. 2016; 134:645–657. DOI: 10.1016/j.neuroimage.2016.04.051 [PubMed: 27118088]

Shakil S, Lee CH, Keilholz SD. Evaluation of sliding window correlation performance for characterizing dynamic functional connectivity and brain states. Neuroimage. 2016; 133:111–128. DOI: 10.1016/j.neuroimage.2016.02.074 [PubMed: 26952197]

Steinley D. Properties of the Hubert-Arabie adjusted Rand index. Psychol Methods. 2004; 9:386–396. DOI: 10.1037/1082-989X.9.3.386 [PubMed: 15355155]

Thompson WH, Fransson P. On stabilizing the variance of dynamic functional brain connectivity time series. Brain Connect. 2016; 6:1–21. DOI: 10.1089/brain.2016.0454 [PubMed: 26414628]

Van Der Maaten LJP, Hinton GE. Visualizing high-dimensional data using t-sne. J Mach Learn Res. 2008; 9:2579–2605. DOI: 10.1007/s10479-011-0841-3

Vergara VM, Mayer AR, Damaraju E, Hutchison K, Calhoun VD. The effect of preprocessing pipelines in subject classification and detection of abnormal resting state functional network connectivity using group ICA. Neuroimage. 2016; 145:365–376. DOI: 10.1016/j.neuroimage. 2016.03.038 [PubMed: 27033684]

Vossel S, Geng JJ, Fink GR. Dorsal and ventral attention systems: distinct neural circuits but collaborative roles. Neuroscience. 2014; 20:150–159. DOI: 10.1177/1073858413494269

Wang J, Yang Y, Fan L, Xu J, Li C, Liu Y, Fox PT, Eickhoff SB, Yu C, Jiang T. Convergent functional architecture of the superior parietal lobule unraveled with multimodal neuroimaging approaches. Hum Brain Mapp. 2015; 36:238–257. DOI: 10.1002/hbm.22626.Convergent [PubMed: 25181023]

Weissman DH, Roberts KC, Visscher KM, Woldorff MG. The neural bases of momentary lapses in attention. Nat Neurosci. 2006; 9doi: 10.1038/nn1727

Xie H, Gonzalez-Castillo J, Damaraju E, Bandettini PA, Calhoun VD, Mitra S. Resting-state functional network connectivity pattern as a cognitive marker for task performance. Presented at the 25th Annual Meeting of ISMRM; Honolulu, USA. April 25 2017; 2017.

Zhang DY, Raichle ME. Disease and the brain's dark energy. Nat Rev Neurol. 2010; 6:15–28. DOI: 10.1038/nrneurol.2009.198 [PubMed: 20057496]
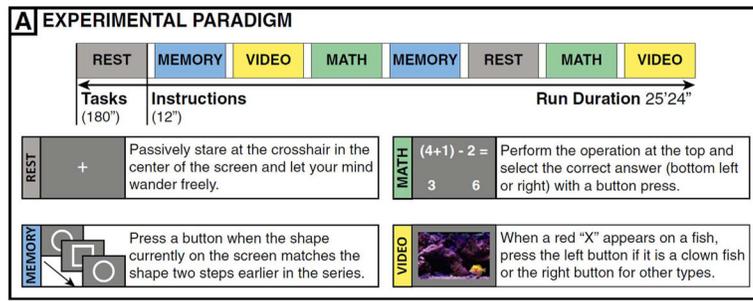
Fig. 1.
The experimental paradigm taken from Gonzalez-Castillo et al. (2015).
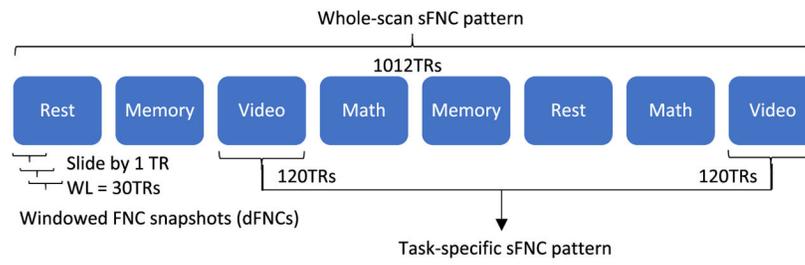
Fig. 2.
Generation of whole-scan, task-specific sFNC and dFNC patterns. Each block consists of 120 time points of 61 ICNs, and sFNC pattern is computed as the temporal correlation between those components and vectorized to a feature vector.
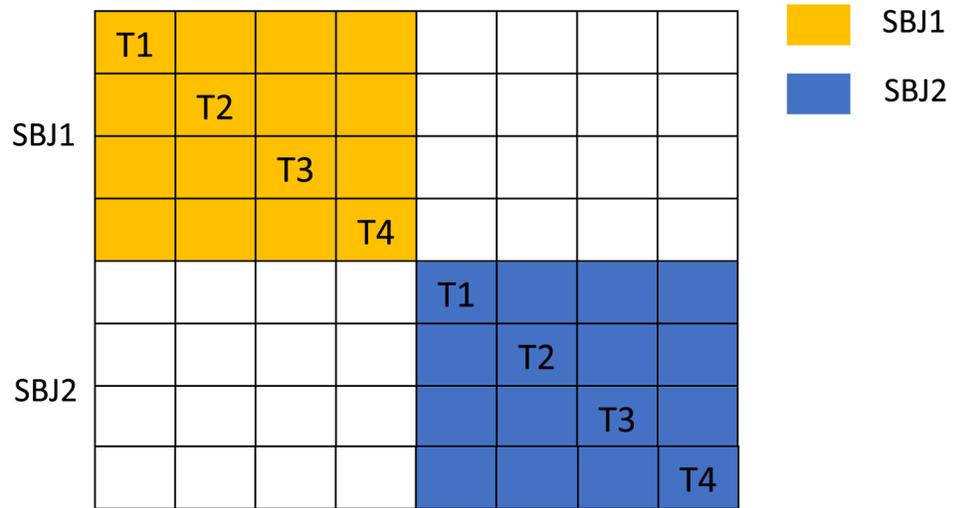
Fig. 3.

Illustration of a similarity matrix and calculation of S_{task} and S_{indiv}. Each block represents a dFNC similarity pair by correlating two dFNC snapshots. $S_{task}(t)$ is the average value of all blocks of a given task, T1 (task 1), T2 (task2), etc. $S_{indiv}(i)$ is the average similarity of each 4×4 block color-coded based on subject identity.
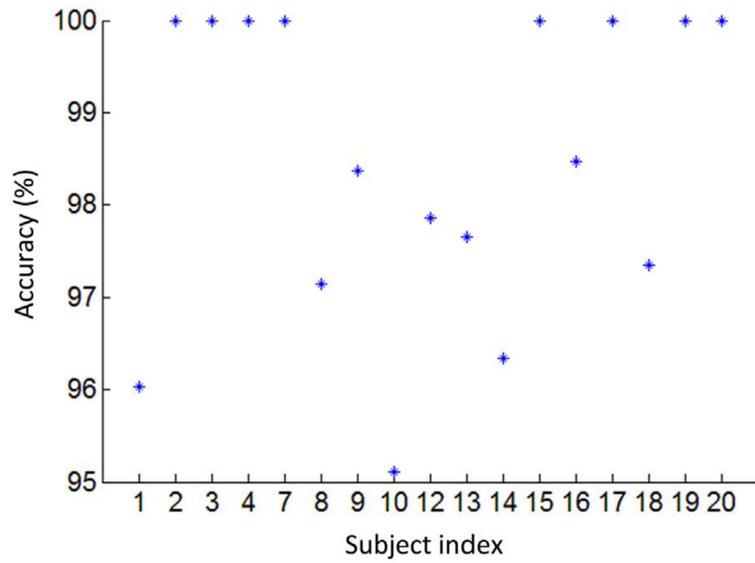
Fig. 4.
Prediction accuracy of subject identity using dFNC snapshots (WL = 30TRs) with the same subject indexes as in the original study (Gonzalez-Castillo et al., 2015).
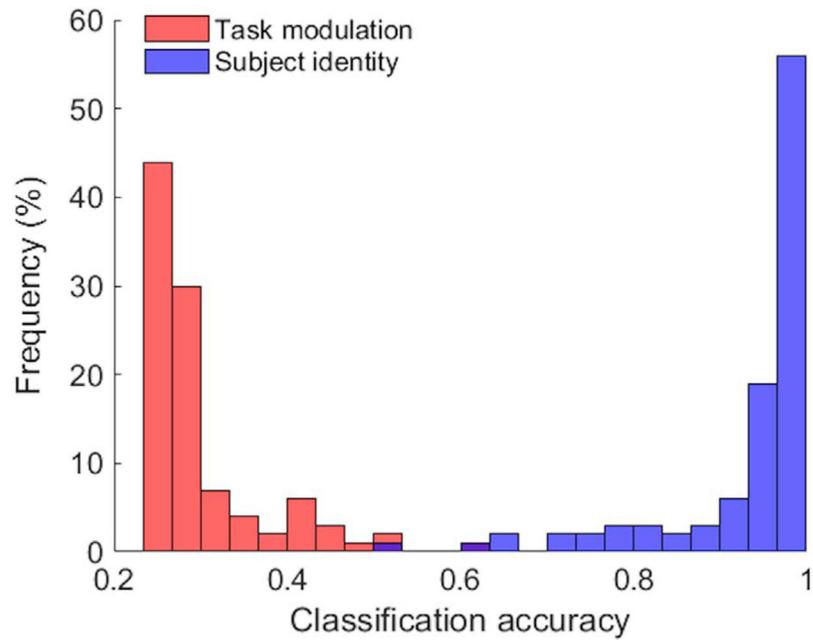
Fig. 5.
Histogram of k-means classification accuracies over 100 repetitions by comparing k-means results with task modulation (red) and subject identity (blue). The average classification accuracy was 29.88% based on task modulation and 93.67% based on subject identity, showing that the resulting partition was dominated by the subject identity (FC individuality) rather than task modulation.
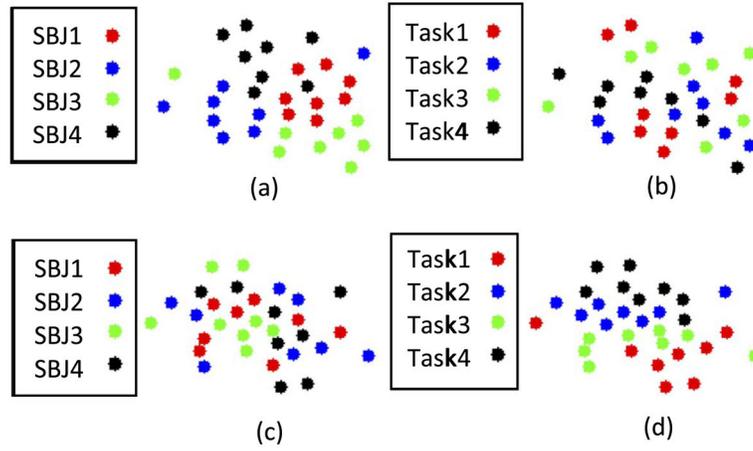
Fig. 6.
t-SNE projection of dFNCs before and after removal of FC individuality. (a) Raw dFNCs colored coded based on subject identity. (b) The same projection as shown in (a), while colored coded based on task modulation. (c) Regressed dFNCs colored coded based on subject identity. (d) The same projection as shown in (c), but colored coded based on task modulation. Note that (a) and (d) are much more structured than (b) and (c).
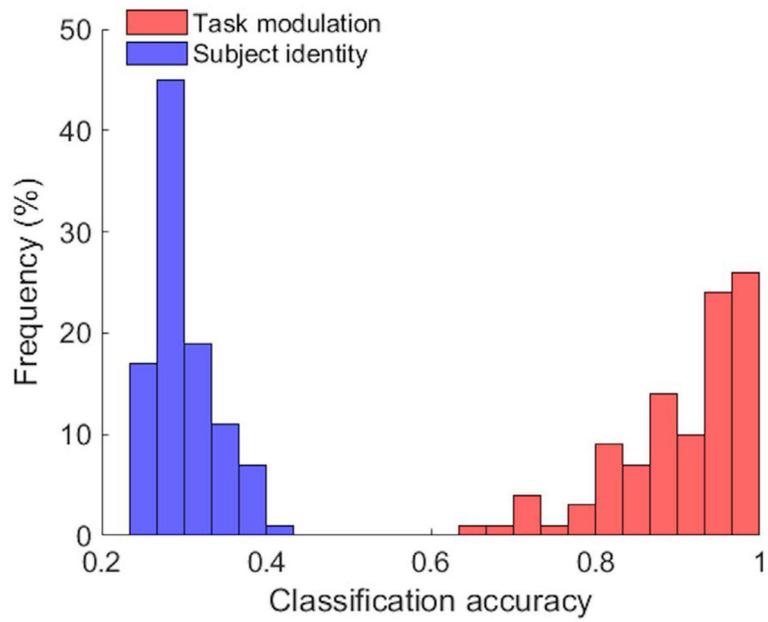
Fig. 7.
Histogram of k-means classification accuracies over 100 repetitions by comparing k-means results with task modulation (red) and subject identity (blue) after the removal of FC individuality. The average classification accuracy was 90.43% based on task modulation and 30.05% based on subject identity, showing that the resulting partition was dominated by task modulation.
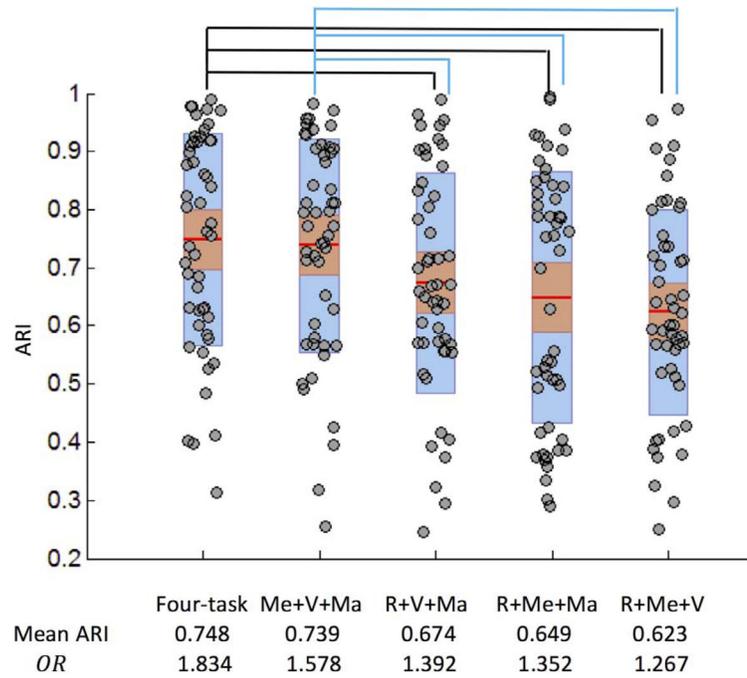
Fig. 8.
Boxplot of ARIs over 50 repetitions based on task modulation after regressing out three-task sFNC patterns and four-task sFNC pattern. The 95% confidence interval is shown in red and mean ± one SD is shown in blue. R: rest; Me: memory; V: video; Ma: math. Mean ARIs and OR_s are highly correlated (p = 0.02). Paired t-test showed significant group difference between the groups denoted (p < 0.01, Bonferroni adjusted).
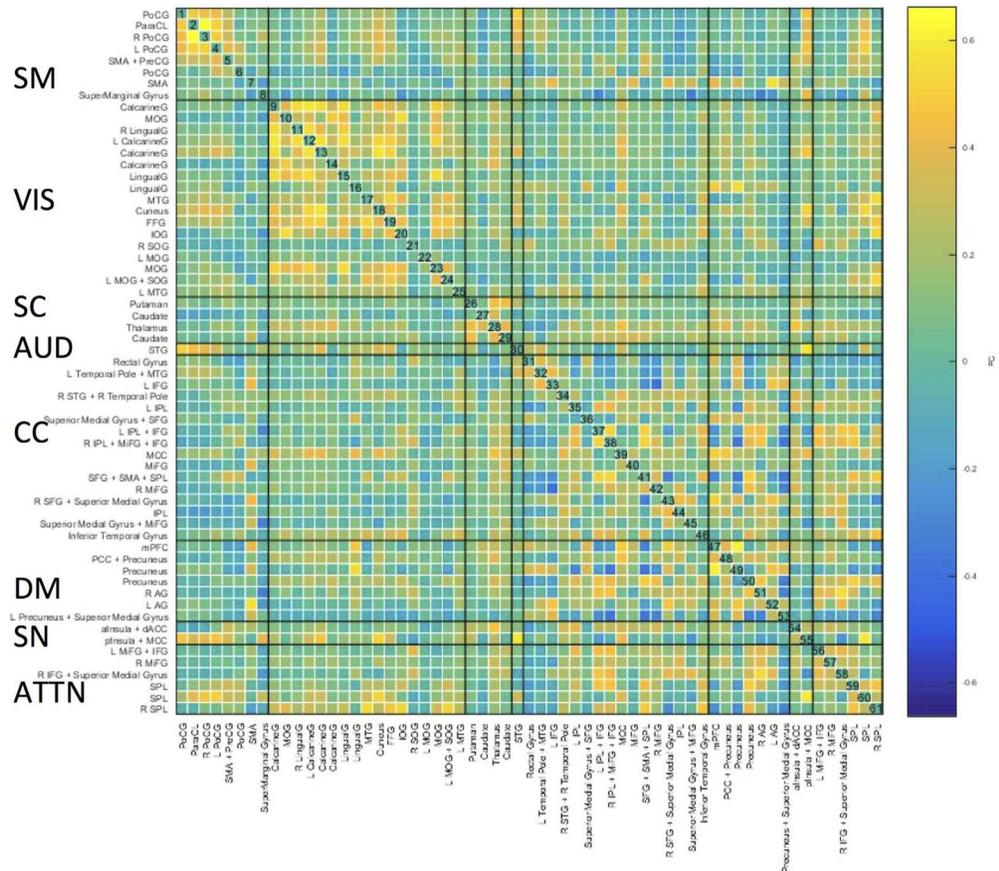
Fig. 9.
Mean of the whole-scan sFNC pattern of thirteen good performers. Coarse anatomic labels for each ICN are shown along the x- and y-axes. SM: sensorimotor; VIS: Visual; SC: subcortical; AUD: auditory; CC: cognitive control; DM: default-mode; SN: salience network; ATTN: attentional network.
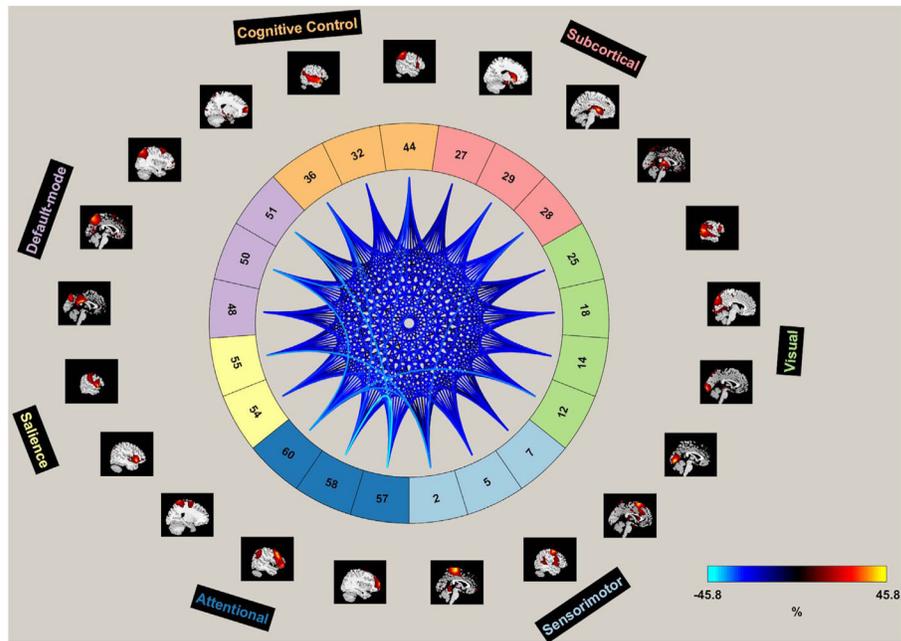
Fig. 10.
Average percentage change of group-level variance of FC dynamics after removing FC individuality. Only the most variable ICNs across subjects (n = 21) are shown with the ICN indexes.

Table 1

Frequency of occurrence of ARIs over 100 repetitions before and after removal of FC individuality. It is observed that before the removal of FC individuality, the recovery of task modulation is either poor or around or below chance-level while the recovery of subject identity is rather good. Such effect is reversed after FC individuality removal.

ARI	Frequency before removal (%)		Frequency after removal (%)	
	Task modulation	Subject identity	Task modulation	Subject identity
Excellent ($0.9 < ARI \leq 1$)	0	65	32	0
Good ($0.8 < ARI \leq 0.9$)	0	15	21	0
Moderate ($0.65 < ARI \leq 0.8$)	0	6	28	0
Poor ($0.1 < ARI \leq 0.65$)	13	14	19	1
Chance-level ($ARI \leq 0.1$)	87	0	0	99

Table 2

ORs using different combinations of sFNC patterns. R: rest; Me: memory; V: video; Ma: math. Higher *OR* represents better revelation of task-induced FC pattern against subject-specific FC profile.

Four-task sFNC Pattern	R + Me + V + Ma	1.834
Three-task sFNC Pattern	Me + V + Ma	1.578
	R + V + Ma	1.392
	R + Me + Ma	1.352
	R + Me + V	1.267
Two-task sFNC Pattern	R + Me	0.857
	R + V	0.906
	R + Ma	1.052
	Me + V	1.001
	Me + Ma	1.145
	V + Ma	1.104
One-task sFNC Pattern	R	0.566
	Me	0.665
	V	0.628
	Ma	0.698

Table 3

Percentage decrease of network-level connectivity variance after FC individuality removal.

Functional network	Decrease of network-level connectivity variance
Salience network	16.51%
Attentional network	15.63%
Subcortical network	14.06%
Cognitive control network	13.42%
Auditory network	12.97%
Default-mode network	12.68%
Sensorimotor network	12.29%
Visual network	12.22%